

# CHEM MED CHEM

CHEMISTRY ENABLING DRUG DISCOVERY

## Accepted Article

**Title:** S-(4-methoxyphenyl)-4-methoxybenzenesulfonothioate as a promising lead compound for the development a renal carcinoma agent

**Authors:** Camila I. Namtes, Ingrid D. Pereira, Ruoli Bai, Ernest Hamel, James C. Burnett, Rodrigo J. de Oliveira, Maria de F. C. Matos, Adilson Beatriz, Murilo K. A. Yonekawa, Renata T. Perdomo, Dênis P. de Lima, Danielle Bogo, and Edson dos Anjos dos Santos

This manuscript has been accepted after peer review and appears as an Accepted Article online prior to editing, proofing, and formal publication of the final Version of Record (VoR). This work is currently citable by using the Digital Object Identifier (DOI) given below. The VoR will be published online in Early View as soon as possible and may be different to this Accepted Article as a result of editing. Readers should obtain the VoR from the journal website shown below when it is published to ensure accuracy of information. The authors are responsible for the content of this Accepted Article.

**To be cited as:** *ChemMedChem* 10.1002/cmdc.201900566

**Link to VoR:** <http://dx.doi.org/10.1002/cmdc.201900566>

WILEY-VCH

[www.chemmedchem.org](http://www.chemmedchem.org)

A Journal of



# S-(4-methoxyphenyl)-4-methoxybenzenesulfonothioate as a promising lead compound for the development of a renal carcinoma agent

Camilla I. Nantes,<sup>[b]</sup> Ingrid D. Pereira,<sup>[c]</sup> Ruoli Bai,<sup>[d]</sup> Ernest Hamel,<sup>[d]</sup> James C. Burnett,<sup>[e]</sup> Rodrigo J. de Oliveira,<sup>[f]</sup> Maria de F. C. Matos,<sup>[b]</sup> Adilson Beatriz,<sup>[c]</sup> Murilo K. A. Yonekawa,<sup>[a]</sup> Renata T. Perdomo,<sup>[b]</sup> Dênis P. de Lima,<sup>[c]</sup> Danielle Bogo,<sup>[b]</sup> Edson dos A. dos Santos\*<sup>[a]</sup>.

- [a] M. K. A. Yonekawa 0000-0002-6613-6467, Prof. E. dos A. dos Santos, 0000-0003-2642-0970  
Laboratório de Bioquímica Geral e de Microorganismos - Instituto de Biociências  
Universidade Federal de Mato Grosso do Sul  
Av. Costa e Silva s/n, Cidade Universitária, CEP 79070-900, Campo Grande – MS, Brazil  
E-mail: edsonanjos@hotmail.com
- [b] C. I. Nantes, Prof. M. de F. C. Matos, 0000-0003-4240-0849, Prof. R. T. Perdomo, 0000-0003-2747-7039, Prof. D. Bogo, 0000-0003-0233-3047  
Laboratório de Biologia Molecular e Culturas Celulares - Faculdade de Ciências Farmacêuticas, Alimentos e Nutrição  
Universidade Federal de Mato Grosso do Sul  
Av. Costa e Silva s/n, Cidade Universitária, CEP 79070-900, Campo Grande – MS, Brazil
- [c] I. D. Pereira, Prof. A. Beatriz, 0000-0001-6864-6092, Prof. D. P. de Lima, 0000-0002-6023-4867  
Laboratório de Pesquisa 4 - Instituto de Química  
Universidade Federal de Mato Grosso do Sul  
Av. Senador Müller, 1555, CEP 79070-900, Campo Grande – MS, Brazil
- [d] R. Bai, Dr. E. Hamel, 0000-0003-3648-103X  
Screening Technologies Branch, Developmental Therapeutics Program, Division of Cancer Treatment and Diagnosis, Frederick National Laboratory  
National Cancer Institute (NCI)  
Frederick, MD 21702, USA
- [e] Dr. J. C. Burnett  
Computational Drug Development Group, Screening Technologies Branch, Developmental Therapeutics Program, Division of Cancer Treatment and Diagnosis, Frederick National Laboratory  
National Cancer Institute (NCI)  
Frederick, MD 21702, USA
- [f] Prof. R. J. de Oliveira, 0000-0003-3514-3346  
Centro de Estudos e Células Tronco, Terapia Celular e Genética Toxicológica  
Universidade Federal de Mato Grosso do Sul, CeTroGen – NHU, Campo Grande (MS), Brazil

Supporting information for this article is given via a link at the end of the document.

**Abstract:** Organosulfur compounds show cytotoxic potential towards many tumor cell lines. Disulfides and thiosulfonates act through apoptotic processes, inducing proteins associated with apoptosis, endoplasmic reticulum stress, and the unfolded protein response. Three *p*-substituted symmetric diaryl disulfides and three diaryl thiosulfonates were synthesized and analyzed for inhibition of tubulin polymerization and for human cancer cell cytotoxic activity against seven tumor cell lines and a non-tumor cell line. S-(4-methoxyphenyl)-4-methoxybenzenesulfonothioate (**6**) exhibited inhibition of tubulin polymerization and showed the best antiproliferative potential, especially against the 786-0 cell line, being six times more selective as compared with the non-tumor cell line. In addition, compound **6** was able to activate caspase-3 after 24 and 48 h treatments of the 786-0 cell line and induced cell cycle arrest in the G2/M stage at the highest concentration evaluated at 24 and 48 h. Compound **6** was able to cause complete inhibition of proliferation, inducing the death of 786-0 cells, by increasing the number of cells at G2/M and greater activation of caspase-3.

## Introduction

The cell cycle and the apoptotic process are important targets for anticancer therapy since tumor growth is associated with the imbalance of cellular proliferation and cell death.<sup>[1-3]</sup> Although many available chemotherapeutic drugs are capable of inducing apoptosis in tumor cells, the majority of them also cause normal cell death, particularly in tissues with high proliferative rates.<sup>[4-5]</sup> A great challenge for antitumor therapies is the genetic heterogeneity of advanced cancer because many cancer cells can develop resistance to chemotherapeutic drugs.<sup>[6]</sup> Metastatic renal cell carcinoma is especially chemoresistant.<sup>[7]</sup> The resistance shown by these cells may be related to their high concentration of intracellular glutathione (GSH).<sup>[8]</sup> Renal carcinoma cells are known for producing a high concentration of intracellular glutathione (GSH).<sup>[9]</sup> This antioxidant protects cells from toxic effects of reactive species of oxygen (ROS) and elimination of xenobiotics. However, disulfides (RS-SR) and thiosulfonates (RS-S(O)<sub>2</sub>R) are able to act significantly through S-thiolation of GSH, leading to its oxidized form (RS-SG).<sup>[10]</sup> This generates an expressive reduction of intracellular GSH and consequently, to the increase of ROS. In addition, it is likely to be linked to the greater expression of genes that encode efflux pumps such as P-glycoprotein and the MPR-1 pumps detected

in clinical samples<sup>[11-12]</sup> and in cultured cells of renal adenocarcinomas, such as the lines ACNH, A-498, and 786-0.<sup>[13]</sup> Clear-cell renal carcinoma is also considered a hypervascular tumor due to inactivation of the suppressor von Hippel Lindau gene that triggers the induction of proangiogenic factors, facilitating metastasis.<sup>[14-15]</sup> All these factors make renal carcinoma an invasive and aggressive tumor.<sup>[9]</sup> Herein, the focus was on some mechanisms responsible for the anticancer activity of many anticancer agents.

Hence, addressing alternative means for renal cancer treatment continues to be an important issue, and the search for new compounds that act selectively in chemoresistant cells is imperative. Compounds containing sulfur present cytotoxic potential against many tumor cell lines.<sup>[10,16-21]</sup> Some that can be highlighted are the disulfide I,<sup>[10]</sup> the thiosulfonate II and, the disulfide III<sup>[21]</sup> that exhibit cytotoxic activity against esophageal cancer cells<sup>[21,10]</sup> (Fig.1). Compounds I and II act by means of stimulation of the S-thiolation protein that leads to endoplasmic reticulum (ER) stress and triggers the unfolded protein response.<sup>[10]</sup> Thiosulfonates and disulfides are general electrophiles and can cause cell death, e.g., S-methyl methanethiosulfonate (MMTS) is a common cysteine alkylating reagent and forms disulfides with cellular cysteines.<sup>[22]</sup> Compound III leads to the induction of proteins associated with apoptosis, such as mitogen-activated kinase (MAPK) by ER stress.<sup>[21]</sup>

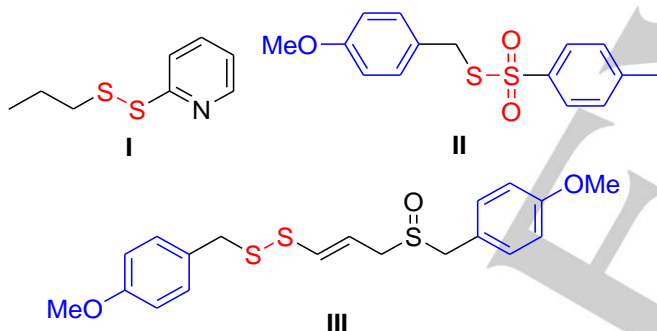


Figure 1. Chemical structures of I, II and III.

The diaryl disulfides (1-3) and diaryl thiosulfonates (4-6) (Figure 2) have structural similarities to the compounds shown in Figure 1. Some of them are known by their biological activities as antimalarial<sup>[23]</sup> (1), leishmanicidal<sup>[24]</sup> (1 and 2), fungicidal<sup>[25]</sup> (1 and 4) and larvicidal<sup>[26]</sup> (5 and 6). Disulfide 1 and the thiosulfonate 4 have cytotoxicity against human leukemia RPMI 8402 cells.<sup>[27]</sup> Disulfide 3 has antiproliferative activity against HEK293 cells (human embryonic kidney) in the same concentrations that they stabilize the tumor suppressor Programmed cell death-4 (Pdc4). The stabilization is regarding to the maintenance of protein Pdc4 expression through the not yet studied mechanisms. The tumor suppression is lost in many different types of tumors and the reduction of this expression acts as prognostic marker in tumorigenesis.<sup>[28]</sup> The cytotoxic activities of this class of compounds, combined with studies of the antiproliferative mechanism of action, inspired us to investigate their behavior as anticancer agents for other tumor cell lines, as well as, the capacity of 6 to trigger tumor cell line

786-0 apoptosis. The compound was selected to be assayed against this cell line since it showed the best results for cytotoxic tests against these cells. Moreover, in spite compound 6 is a known compound, it had not been tested for antitubulin activity.

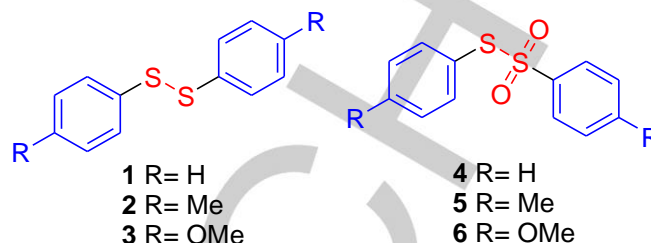


Figure 2. Chemical structures of diaryl disulfides 1-3 and diaryl thiosulfonates 4-6.

## Results and Discussion

### Synthesis

Diaryl disulfides (1-3) and diaryl thiosulfonates (4-6) were prepared as shown in Scheme 1. The diaryl disulfides (1-3) were formed via oxidative coupling of thiols, with yields ranging from 25 to 71 % together with 4-6 with yields ranging from 9 to 22 %.



Scheme 1. Synthesis of diaryl disulfides (1-3) and diaryl thiosulfonates (4-6).

The diaryl sulfides (1-3) were synthesized in good yields through a methodology adapted from Santos and coworkers.<sup>[26]</sup> Heating the reaction mixtures under reflux led to formation of thermodynamic controlled disulfides as the major products. IR, <sup>1</sup>H-NMR, <sup>13</sup>C-NMR and HR-ESI-MS spectra of the synthesized compounds (1-6) are available in the Support Information.

### Biological tests

#### Inhibitory effects on tubulin polymerization

Compounds 1-6 were evaluated for effects on the polymerization of purified tubulin and on the inhibition of [<sup>3</sup>H]colchicine binding to tubulin. Combretastatin A-4 (CSA4) (Figure 3) was used as a positive control, and the results are shown in Table 1. In the assembly assay, all six compounds showed significant antitubulin activity. Compound 3 showed the highest activity (IC<sub>50</sub>= 1.4 μM), followed by 1 (IC<sub>50</sub>= 1.8 μM), 6 (IC<sub>50</sub>= 2.3 μM) and 5 (IC<sub>50</sub>= 2.5 μM), while compounds 4 and 2 were less active, with IC<sub>50</sub> values of 3.5 and 6.3 μM, respectively. Compounds 3 and 6 (Scheme 1) were the only ones bearing a methoxy substituent in both aromatic rings. This feature is often considered critical for compounds to bind at the colchicine site of tubulin.<sup>[17,29]</sup> Previously, we described the synthesis of disulfide 7

(Figure 3), which inhibited tubulin assembly with an  $IC_{50}$  of  $5.4 \pm 0.4 \mu\text{M}$ , the first indication that disulfides can be effective antitubulin agents.<sup>[17]</sup>

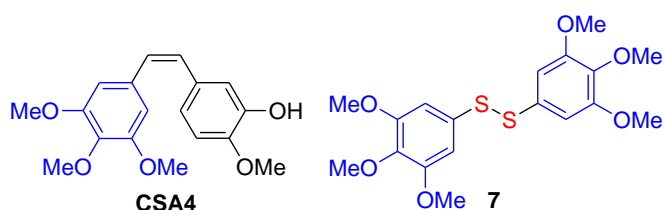


**Figure 3.** Chemical structures of combretastatin A-4 (CSA4) and bis(3,4,5-trimethoxyphenyl) disulfide (7).

Even though the compounds had significant activity as inhibitors of tubulin assembly, they were significantly less active than CSA4. When evaluated for effects on the binding of [<sup>3</sup>H]colchicine to tubulin, this reduced activity compared with CSA4 was even more dramatic. Most notably, perhaps, the best inhibitor of assembly, compound **3**, had only weak inhibitory effects on colchicine binding (Table 1), most likely caused by poor solubility in the reaction mixture.

Compounds **5** and **6** showed the best inhibition of colchicine binding to tubulin with 40 and 39 % inhibition, respectively, at a concentration of  $5 \mu\text{M}$ . The four less active compounds in the colchicine assay were also evaluated at  $50 \mu\text{M}$ , and at this higher concentration, compound **4** showed the strongest inhibition (82 %).

Often, either effects on tubulin polymerization or, especially, effects on ligand binding, can be correlated with cytotoxic effects.<sup>[30-32]</sup> However, this does not appear to be the case with compounds **1-6**. Neither the mean  $GI_{50}$  of the seven cancer cell lines (95, 109, 68, 119, 98 and  $43 \mu\text{M}$ , for compounds **1-6**, respectively) nor those of any individual line showed significant correlation with the antitubulin activities of the compounds. Nevertheless, the lowest mean  $GI_{50}$  values were obtained with compounds **3** and **6**, which had the greatest effects on assembly and on colchicine binding, respectively.

**Table 1.** Compound effects on tubulin polymerization and the binding of colchicine to tubulin.

Compounds	Tubulin polymerization $IC_{50}^{[a]}$ ( $\mu\text{M}$ ) $\pm$ SD	Inhibition of binding of colchicine, % inhibition $\pm$ SD	
		$5 \mu\text{M}$ inhibitor	$50 \mu\text{M}$ inhibitor
CSA4 <sup>[b]</sup>	$0.54 \pm 0.06$	$100 \pm 0.4$	NT <sup>[c]</sup>
<b>1</b>	$1.8 \pm 0.1$	$10 \pm 5$	$15 \pm 4$
<b>2</b>	$6.3 \pm 1$	$9.9 \pm 5$	$25 \pm 5$
<b>3</b>	$1.4 \pm 0.2$	$29 \pm 1$	$47 \pm 1$
<b>4</b>	$3.5 \pm 0.3$	$4.0 \pm 3$	$82 \pm 5$
<b>5</b>	$2.5 \pm 0.3$	$40 \pm 3$	NT
<b>6</b>	$2.3 \pm 0.1$	$39 \pm 0.8$	NT

[a]  $IC_{50}$  is the concentration inhibiting the extent of tubulin polymerization by 50 % after 20 min at  $30 \text{ }^\circ\text{C}$ . [b]  $IC_{50}$  for inhibition of tubulin assembly and % inhibition of binding of colchicine for CSA4 were obtained contemporaneously with the values for all compounds; [c] NT: not tested.

To generate a structure-based hypothesis for the reduced colchicine binding inhibition of compound **6** versus CSA4, molecular docking studies were performed. Compound **6** was chosen as the thiosulfonate derivative for docking since it generally had the strongest antiproliferative activity of compounds **1-6** (Table 2), and all subsequent biochemical data shown in Figures. 5-9 focuses on this derivative.

### Molecular docking studies

The atomic coordinates used to generate the model were obtained from publicly available PDB entry 5LYJ, a tubulin-CSA4 co-crystal that was described in 2017. As shown in Figure 4A, compound **6** possesses key pharmacophore features for colchicine binding site inhibitors, as described by Nguyen et al.<sup>[33]</sup> However, unlike CSA4, compound **6** lacks the hydroxyl substituent on ring A, but it does incorporate a hydrogen bond accepting group in the central thiosulfonate moiety (Figure 4A).

An energy refined model of the tubulin-CSA4 co-crystal structure (Figure 4B), in agreement with the biochemical data, indicates that the inhibitor binds in the colchicine site with good steric complementarity, engages in hydrogen bonds with the side chain thiol of Cys 241 and the backbone carbonyl oxygen of Thr 179, and participates in favorable hydrophobic contacts with surrounding residues Leu 248, Ala 250, Leu 255 (not shown for image clarity), Met 259 (not shown for image clarity), Ala 316, and Ile 378. The quantitated Glide (Maestro, Schrödinger, LLC, New York, NY) score for the bound inhibitor was -8.6, which indicates favorable binding. The weaker binding mode for compound **6** (Glide score = -6.6) is shown in Figure 4C and provides a basis for rationalizing the weaker colchicine site inhibition of the thiosulfonate derivatives, in general, versus CSA4.

Specifically, as shown in Figure 4C, the lack of a hydroxyl group substituent on ring A of **6** results in the loss of a strong hydrogen bond ( $2.4 \text{ \AA}$  distance) with the backbone carbonyl oxygen of residue Thr 179 that is observed in the CSA4 binding mode. However, this lost hydrogen bond is partially compensated for by the formation of a weaker hydrogen bond ( $3.0 \text{ \AA}$ ) between one of the thiosulfonate oxygens and the side chain amide nitrogen of Asn 258. Furthermore, the lack of methoxy groups on the 3 and 4 positions of ring B (Figure 4A) decreases the number of favorable hydrophobic contacts between compound **6** and surrounding hydrophobic residues (e.g., Leu 248 and Ala 316), and therefore its steric occupancy in this location of the colchicine site is reduced versus CSA4. However, based on the model, the most striking reason for the reduced potency of compound **6** is that the thiosulfonate-mediated increase in bond distance between rings A and B ( $2.2 \text{ \AA}$ , Figure 4A), versus a corresponding distance of the  $1.4 \text{ \AA}$  in CSA4 (Figure 4A), places the ring A 4-methoxy substituent methyl of **6** within unfavorable hydrophobic-polar distances to the backbone carbonyls of Asn 350 ( $3.4 \text{ \AA}$ ) and Asn 258 ( $3.3 \text{ \AA}$ ) (Figure 4C). Such close intermolecular proximities between hydrophobic and polar groups/atoms are not observed in high resolution protein-small molecule co-crystal structures. In CSA4, the corresponding

distances are within the tolerated norms of 3.8 Å and 4.5 Å, respectively. Finally, Figure 4D provides a reference graphic for the general context of the CSA4 and compound **6** binding poses described above.

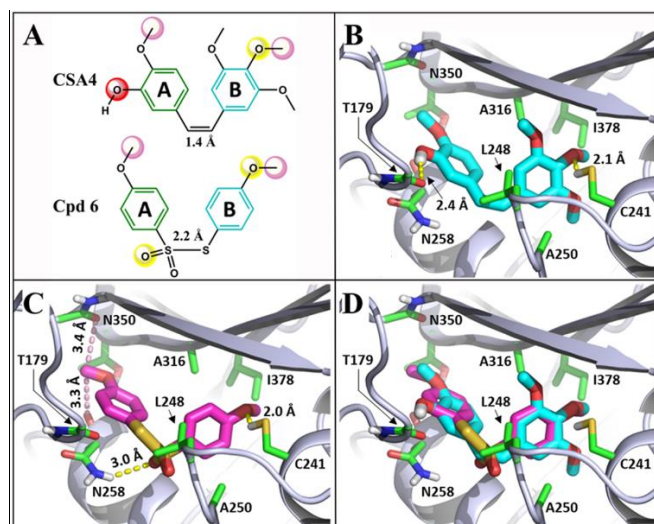


**Figure 4.** Comparison of the binding modes of CSA4 and compound **6**. A) Pharmacophore requirements for colchicine site binding.<sup>[33]</sup> Pink spheres indicate hydrophobic points, red spheres indicate hydrogen bond donors, and yellow spheres indicate hydrogen bond acceptors. Green (ring A) and cyan

(ring B) indicate key aromatic components forming the core scaffold for colchicine site binding. B) The energy refined binding mode of colchicine (bluewhite cartoon) - CSA4 co-crystal structure PDB entry 5LYJ. CSA4 carbons are cyan, residue carbons are green, and hydrogen bond distances are shown with yellow dash. C) Modeled binding mode of compound **6** (magenta carbons). Residue carbons are green, and hydrogen bond distances are shown with yellow dash, and unfavourable hydrophobic-polar distances are shown with pink dash. D) Superimposed binding modes of CSA4 and compound **6**. All carbon colors are as indicated in B and C (above).

#### Antiproliferative activities

The cytotoxic activity of the organosulfur compounds against B16-F10, PC-3, HT-29, 786-0, MCF-7, MDA-MB-231, and HEPG2 tumor cell lines and against the NIH/3T3 non-tumor cell line were evaluated by the colorimetric SRB assay in three independent experiments. The results are expressed as  $GI_{50}$  ( $\mu\text{M}$ ) values (Table 2). All evaluated organosulfur compounds had moderate activity ( $GI_{50}$  10-100  $\mu\text{M}$ ) for at least one tumor cell line. Compound **6** showed the best antiproliferative potential, exhibiting moderate activity against all cell lines with the lowest  $GI_{50}$  values for the 786-0 (ATCC-CRL-1932) and MDA-MB-231 cell lines. Compound **6** had the greatest activity against the 786-0 cell line ( $GI_{50}$  9.08  $\mu\text{M}$ ). In these studies, doxorubicin was used as the positive control.

**Table 2.** Antiproliferative activity of organosulfur compounds against tumor cell lines and non-tumor NIH/3T3 cell line.

Compounds	$GI_{50}$ ( $\mu\text{M}$ ) $\pm$ SEM							
	B16-F10	PC-3	HT-29	786-0	MCF-7	MDA-MB-231	HEPG2	NIH/3T3
1	100.0 $\pm$ 7.08	110.5 $\pm$ 3.40	109.0 $\pm$ 0.54	111.6 $\pm$ 0.52	105.6 $\pm$ 2.04	61.97 $\pm$ 28.20	66.94 $\pm$ 28.58	55.64 $\pm$ 9.75
2	101.2 $\pm$ 0.07	112.3 $\pm$ 6.51	168.6 $\pm$ 49.79	146 $\pm$ 2.90	89.29 $\pm$ 2.79	102.6 $\pm$ 2.83	46.35 $\pm$ 19.25	128.9 $\pm$ 18.64
3	20.72 $\pm$ 5.03	69.77 $\pm$ 4.36	171.6 $\pm$ 12.30	18.25 $\pm$ 2.50	89.19 $\pm$ 1.70	86.23 $\pm$ 4.16	19.44 $\pm$ 5.18	186.4 $\pm$ 35.56
4	95.29 $\pm$ 3.29	109.4 $\pm$ 2.11	160.3 $\pm$ 30.17	127.7 $\pm$ 12.50	113.9 $\pm$ 6.14	126.0 $\pm$ 2.29	100.3 $\pm$ 0.68	340.9 $\pm$ 10.20
5	82.57 $\pm$ 0.23	89.84 $\pm$ 0.15	114.6 $\pm$ 15.49	98.89 $\pm$ 1.53	97.09 $\pm$ 5.60	173.3 $\pm$ 39.05	27.19 $\pm$ 2.10	61.14 $\pm$ 7.21
6	28.59 $\pm$ 0.29	77.22 $\pm$ 0.50	86.47 $\pm$ 11.71	9.08 $\pm$ 0.23 <sup>[b]</sup>	55.77 $\pm$ 1.12	17.89 $\pm$ 5.09	25.13 $\pm$ 0.19	62.53 $\pm$ 0.51
DOXO <sup>[a]</sup>	0.10 $\pm$ 0.06	0.47 $\pm$ 0.04	0.46 $\pm$ 0.01	0.05 $\pm$ 0.00	0.04 $\pm$ 0.00	0.45 $\pm$ 0.04	0.16 $\pm$ 0.06	1.42 $\pm$ 0.05

[a] Doxorubicin; [b]  $GI_{50}$  < 10  $\mu\text{M}$ . Cell lines (human, unless otherwise indicated): B16-F10 (murine melanoma), PC-3 (prostate adenocarcinoma), HT-29 (colorectal adenocarcinoma), 786-0 (renal cell adenocarcinoma), MCF-7 (breast adenocarcinoma), MDA-MB-231 (triple resistant breast), HEPG2 (hepatocellular carcinoma) and NIH/3T3 (murine fibroblast).

Disulfides and thiosulfonates possess antitumor activity.<sup>[34-36]</sup> The capacity of these compounds to form bonds with cell proteins by modifying protein dynamics can interrupt the cell cycle and thus trigger apoptosis.<sup>[37]</sup> Frequently, apoptosis is unleashed by the intrinsic pathway activated by intracellular stress conditions.<sup>[38-40]</sup> Studies performed by Wang and coworkers (2001) showed that diaryl disulfide (**1**) and the thiosulfonate (**4**) were cytotoxicity against human leukemia RPMI 8402 cells, stimulating DNA scission mediated by type II topoisomerase (TOP2) via S-thiolation.<sup>[26]</sup> In our results, such compounds were weakly cytotoxic ( $GI_{50}$  > 50 $\mu\text{M}$ ) in comparison to compounds **3** and **6** whatever the cell lines were tested. As DOXO is strongly cytotoxic for all cell lines, it is not probable that

the mechanism of action of all prepared compounds is resulting from TOPO II inhibition, as it happens for DOXO. In spite of disulfide **3** has been identified as Pdc4 stabilizer in HEK293 cells as reported,<sup>[27]</sup> in our work we can not state that exists a relationship between the activity of compound **3** with the stabilization of Pdc4 in 786-0 cells, since we have not performed the assays. Probably, these compounds target microtubules since **3** and **6** are found to be the most cytotoxic in all cell lines. Besides, organosulfur compounds can provoke microtubule damage by interfering in the polymerization dynamics of tubulin.<sup>[17,41-42]</sup> Compound **5** could be an exception, merely due to membrane permeability problems or underlying

cell resistance mechanisms, notably by a deactivation by the GSH pathway, and not necessarily by the Pgp or MRP-1 protein. Table 3 shows the SI values for each tested compound. SI values were determined in order to establish whether the compounds were more active against a non-tumor cell line in relation to a tumor cell line, in this case, ( $GI_{50}$  NIH/3T3 /  $GI_{50}$  tumor cells). The value for a compound is meaningful when the compound is at least twice as active against tumor cells, *i.e.*,  $SI \geq 2.0$ .<sup>[43]</sup> Compounds **3** and **4** showed significant selectivity ( $SI \geq 2$ ) for all cell lines. The highest values were for compound **3** on the B16-F10 ( $SI=9$ ), 786-0 ( $SI=10.2$ ), HEPG2 ( $SI=9.58$ ) cell lines and compound **6** on 786-0 cell line ( $SI=6.88$ ).

**Table 3.** SI of organosulfur compounds.

Compounds	Cell lines						
	B16-F10	PC-3	HT-29	786-0	MCF-7	MDA-MB-231	HEPG2
<b>1</b>	-	-	-	-	-	-	-
<b>2</b>	1.27	1.15	-	-	1.44	1.26	2.78*
<b>3</b>	9.00*	2.67*	2.36*	10.20*	2.02*	2.16*	9.58*
<b>4</b>	3.58*	3.11*	2.13*	2.67*	3.00*	2.70*	3.4*
<b>5</b>	-	-	-	-	-	-	2.25*
<b>6</b>	2.19*	-	-	6.88*	1.12	3.49*	2.49*

(\*) Values  $\geq 2.0$ : significant SI; 1–2: non-significant SI; (-): absence of selectivity. Cell lines: As described in Table 2.

With exception of **1** and **5**, all other compounds showed good SI for different neoplastic cell lines, suggesting potential for *in vivo* studies. Organosulfur molecules are reported to pose low cytotoxicity against non-tumor cells and show high activity against tumor cells.<sup>[44]</sup>

In this work, we showed that the effectiveness of the synthesized compounds seems to be linked to the aromatic substituent groups. Compounds **3** and **6** showed the best antiproliferative activity and highest SI. The presence of the aryl-OMe fragment in these molecules has been reported as an important feature for increasing cytotoxic activity of different compounds.<sup>[16-17]</sup>

#### Compound **6** showed concentration- and time-dependent antiproliferative activity against the 786-0 cell line

Compound **6** had the highest antiproliferative activity against the 786-0 cell line and was therefore examined for its cytotoxicity (SRB test) for three different time periods. Figure 5 shows the percentage (%) of 786-0 cell line growth after treatment with compound **6** at four concentrations and in periods of 12, 24 and 48 h. At lower concentrations (0.25 and 2.5  $\mu\text{g/mL}$ ), the compound showed antiproliferative activity after 48 h. Starting at concentration of 2.5  $\mu\text{g/mL}$ , the antiproliferative activity increased following the concentration and treatment time,

showing dose-dependent effects. At 2.5  $\mu\text{g/mL}$ , it was active in all time periods. At the highest concentration tested in all experiments (250  $\mu\text{g/mL}$ ), the compound caused cell death.

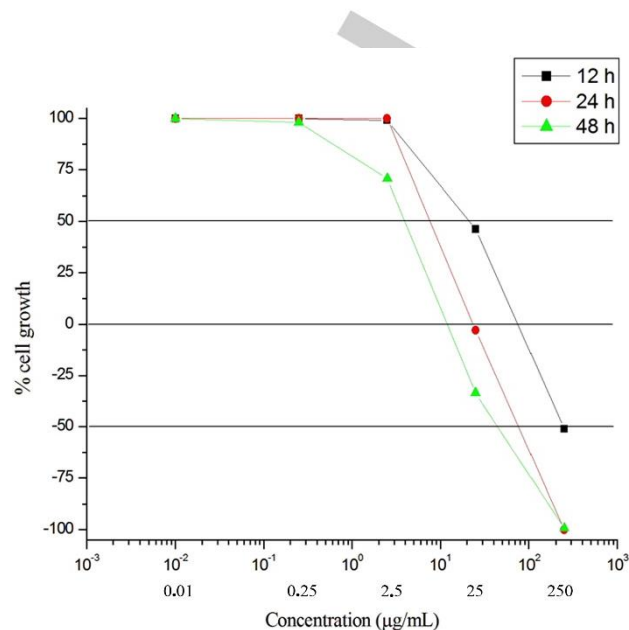


**Figure 5.** *In vitro* antiproliferative activity of compound **6** against the 786-0 cell line in three different time periods. The cells were treated at four concentrations (0.25; 2.5; 25 and 250  $\mu\text{g/mL}$ ) and for 12, 24 or 48 h.

Additionally, compound **6** exhibited the best antiproliferative potential among all tested compounds. Its cytotoxic activity against the 786-0 cell line is concentration- and time-dependent. The  $GI_{50}$  values against the 786-0 cell line in periods of 12, 24 and 48 h were 24.40, 17.40 and 2.82  $\mu\text{g/mL}$ , respectively. At 24 h 25  $\mu\text{g/mL}$ , it showed excellent activity, being able to completely inhibit the proliferation of the 786-0 cell line and induce significant cell death.

#### Compound **6** induces morphological alterations as well as cell death in 786-0 tumor cells

In order to learn if the cytotoxic activity of compound **6** against the 786-0 cell line was associated with apoptosis or necrosis, we performed the differential colorization assay with acridine orange/ethidium bromide (AO/EB). The results of morphological analysis by fluorescence microscopy are shown in Figure 6. At the concentrations of 25  $\mu\text{g/mL}$  after 24 or 48 h treatments, compound **6** caused a significant increase ( $P < 0.01$ ) in the percentage of apoptotic cells, and, at all concentrations, there was a significant increase in apoptosis at different time periods. Cell necrosis was not observed as a result of treatment with compound **6**.

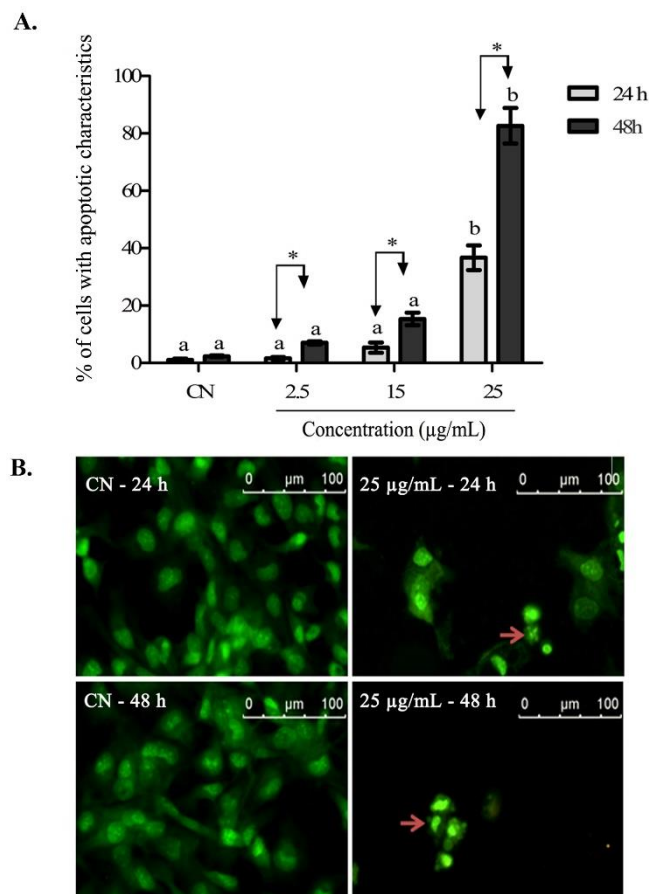


**Figure 6.** Effect of compound **6** on the morphology of 786-0 cells analyzed by AO/EB (acridine orange/ethidium bromide). The non-treated 786-0 cells were used as CN (control negative). For apoptosis assays we used excitation wave of 420-490 nm and barrier filter of 520 nm. (A) Bar graph showing the percentage of cells with apoptotic characteristics after treatment with compound **6** at concentrations of 2.5, 15 or 25 µg/mL for 24 (grey bars) or 48 h (black bars). The values represent the means  $\pm$  SEM of three experiments. Different letters indicate statistical difference ( $P < 0.01$ ) between the experimental times of the same treatment (ANOVA/Tukey), and brackets with asterisks (\*) indicate statistical difference ( $P < 0.01$ ) between the experimental times of the same treatment (Student's unpaired t-test). (B) Fluorescence microscopy image of the non-treated 786-0 cell line and cells treated with compound **6** at 25 µg/mL for 24 or 48 h. The arrows indicate apoptotic cells. Apoptotic cells show green nucleus and apoptotic bodies.

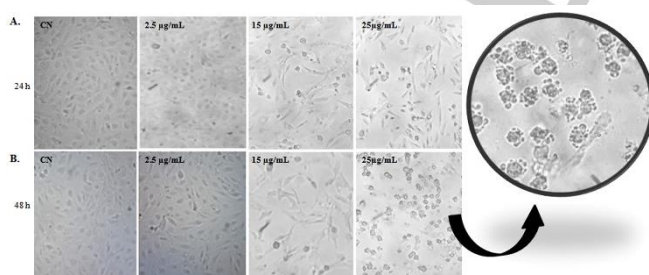


**Figure 7.** Optical microscopy image of non-treated 786-0 cells (CN) and of cells treated with compound **6** at three concentrations (2.5, 15 and 25 µg/mL) for 24 (A) or 48 h (B).

Compound **6** activates caspase-3

Activation of caspase-3 was measured by flow cytometry to confirm the apoptosis induction observed in the morphological studies. After a 24 or 48 h treatment, there was a marked increase of caspase-3 in 786-0 cells treated with compound **6** at concentrations of 2.5, 15 and 25 µg/mL (Figure 8). Compared with untreated control cells, after treatment with 15 µg/mL of compound **6**, there was an increase of 26 and 39 % in caspase-3 levels following treatment for 24 or 48 h, respectively. At 25 µg/mL, the percentage increased to 55 and 76 % in the two periods, respectively. In the treatment at 15 µg/mL there was a significant increase of caspase 3 without time difference of treatment. On the other hand, increasing the concentration to 25 µg/mL, and the treatment time, positively contributed to proportion of activated caspase-3.

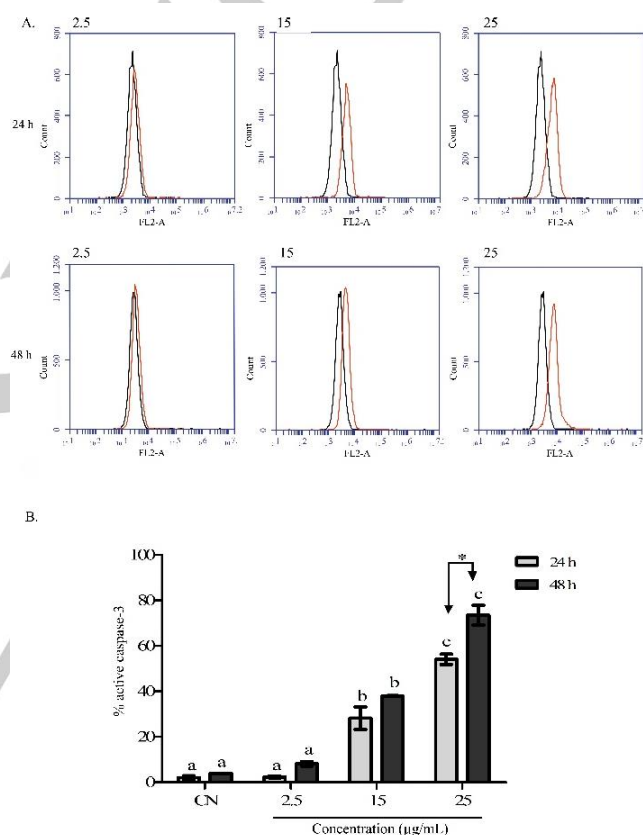


**Figure 8.** Compound **6** effect on the activation of caspase-3 in 786-0 cells. (A) Histograms of fluorescence intensity of flow cytometry; black peaks correspond to the fluorescence of negative control (non-treated cells), red peaks indicate the fluorescence and quantification of caspase-3 in the cells treated with compound **6** at concentrations of 2.5, 15 or 25 µg/mL for 24 or 48 h. (B) Bar graphs correspond to % active caspase-3. The non-treated 786-0 cells were used as CN (control negative). The statistical differences between the treatments of the same experimental time (bars of the same color) were analyzed by (ANOVA/Tukey). Different letters denote significant difference ( $P < 0.01$ ). Brackets with asterisks (\*) indicate significant difference ( $P < 0.01$ ) between the times of the same treatment (Student's unpaired t-test).

Compound **6** induces G2/M phase cell cycle arrest in 786-0 cells

To examine effects on the cell cycle from treatment of cells with compound **6**, the 786-0 cell line was treated with different concentrations of the compound, and the cells were examined by flow cytometry. Cellular DNA was labeled with 7-

aminoactinomycin D (7-AAD), and the percentages of cells in G1, S and G2/M were determined. The histograms shown in Figure 9 show cells that were not treated as well as cells treated with three concentrations of compound **6** at two time points. There was a significant increase ( $P < 0.05$ ) of cells in the G2/M phase when they were treated with compound **6** at 25  $\mu\text{g/mL}$  for 24 or 48 h, with a significant reduction of cells in phase G1 at 48 h.

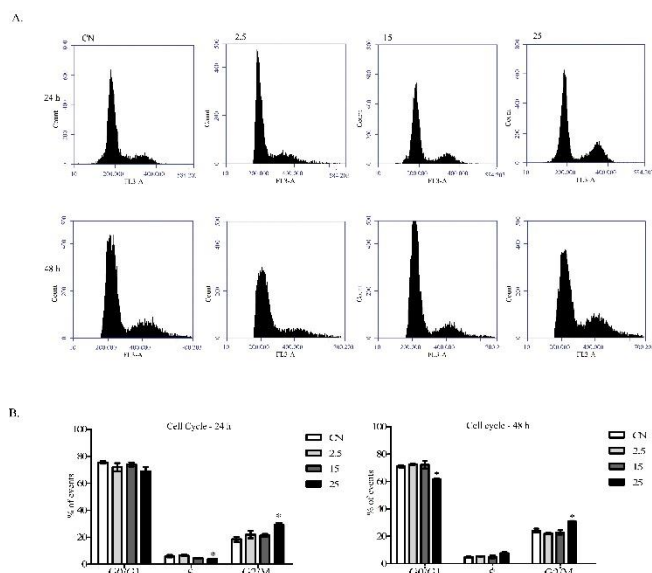


**Figure 9.** Effect of compound **6** on cell cycle progression. (A) Histograms of fluorescence intensity of 786-0 cells labeled with 7-AAD and analysis of G1, S and G2/M phases of non-treated (CN) and treated cells with compound **6** at the concentrations of 2.5, 15 and 25  $\mu\text{g/mL}$  at 24 and 48 h. Analysis of variance (ANOVA) followed by Dunnett's test was performed to evaluate significant differences between the data ( $P < 0.05$ ) obtained without compound and with **6** at the same time points.

Compound **6** caused, under the same experimental condition, an increase in G2/M phase cells and high activation of caspase-3, suggesting a cell cycle arrest and death by apoptosis, since caspase-3 is an effector protease of the apoptosis process that triggers a series of intracellular events resulting in cell death.<sup>[45]</sup> Our experiments showed that diaryl disulfides and diaryl thiosulfonates were capable of inhibiting the polymerization of tubulin. Based on our findings and other reported studies, these sulfur-containing substances interact with intracellular thiol groups in tubulin.<sup>[41-42]</sup> It has been suggested that the interruption of the cell cycle at the G2/M phase might be connected with antitubulin activity since the compounds that interact with microtubules interfere in the formation of the mitotic spindle and thus activate the spindle checkpoint. This results in a block in the cell cycle before the two daughter chromosomes divide.<sup>[46-47]</sup> Compounds that target microtubules and disrupt the normal function of the mitotic spindle have proven to be one of the best classes of cancer chemotherapeutic drugs since they are essential in several cellular functions.<sup>[48]</sup> In addition, these molecules can provoke vascular disruption in tumor cells, acting as antiangiogenic agents.<sup>[49]</sup>

## Conclusions

The synthesized diaryl disulfides and diaryl thiosulfonates inhibited tubulin polymerization, which was greatest with the disulfides **1** and **3** and the thiosulfonate **5** and **6**. Compounds **3** and **6**, bearing methoxy substituents on the aromatic rings, showed the best antiproliferative activity and the best SI values. Compound **6** demonstrated the best antiproliferative potential of all tested organosulfur compounds, showing a low  $\text{GI}_{50}$  against renal carcinoma 786-0 cells. This compound led to complete inhibition of proliferation of 786-0 cells and triggered cell death by increasing the number of cells in the G2/M phase. As observed, phase G2/M cell cycle arrest is directly involved in the inhibition capacity of tubulin polymerization, which is essential for microtubule dynamics during mitosis. The cycle arrest resulted in activation of the caspase-3, leading to apoptosis. Consequently, compound **6** merits attention as a candidate for anticancer therapy in renal cell carcinoma since inhibits 786-0 cell growing. In addition, the compound is selective to NIH/3T3 non-tumor cell line. As renal cell carcinoma is hypervascular tumor, it is highly affected by antitubulin agents. Comparing to the other compounds, it is important to note that compound **6** activity is intimately related to the presence of methoxyl group. For this reason, future proposals should consider to preserve this basic carbon skeleton in order to discover novel and, eventually, more active compounds.

## Experimental Section

### Chemistry

The benzenethiols 4-methylbenzenethiol and 4-methoxybenzenethiol were purchased from Sigma-Aldrich Chemicals (Sigma-Aldrich Corp., St. Louis, MO, USA) or Merck Chemicals (Merck KGaA, Darmstadt, Germany). The melting points of the compounds were determined using a Quimis® 0340S23 melting point apparatus. TLC analyses were performed on aluminum plates coated with silica gel 60 F<sub>254</sub>. Compounds on the plates were visualized using UV light (254 nm). High-resolution mass spectroscopy (HRMS) was performed on a UFLC Shimadzu LC-20AD apparatus with an IES-Q-QTOF-microTOF III detector (Bruker Daltonics) in chemical ionization positive ion mode ( $m/z$  120-1200). Chromatographic purification was performed on silica gel (Merck 100-200 mesh) and analytical TLC on silica gel 60-F<sub>254</sub>, with the compounds detected by fluorescence. <sup>1</sup>H NMR (300 MHz) and <sup>13</sup>C NMR (75 MHz) spectra were recorded on a DPX-300 Bruker instrument and calibrated with residual nondeuterated solvent as an internal reference. Chemical shifts are reported in ppm using tetramethylsilane (TMS) as the internal standard ( $\delta = 0$  ppm), and the coupling constants ( $J$ ) are expressed in Hertz. Infrared spectra were recorded on a FTIR MB100 Boomen in KBr pellets for solids and the absorption wave numbers expressed in  $\text{cm}^{-1}$ . The solvents employed in the reactions and purification processes of the synthesized compounds were distilled and dried.

### General procedure for the synthesis of diaryl disulfides (1-3) and diaryl thiosulfonates (4-6)

To a round-bottomed flask (15 mL) was added the thiol (32 mmol),  $\text{Al}(\text{H}_2\text{PO}_4)_3$  (0.16 mmol) and concentrated  $\text{HNO}_3$  (3 mL). The reaction mixture was stirred under reflux for 2 h and monitored by TLC (hexane/ethyl acetate 9.5:0.5; UV 254 nm). The mixture was transferred to a separatory funnel, and it was extracted with ethyl acetate (70 mL). The pH was raised to 7 by slowly adding a solution of  $\text{NaHCO}_3(\text{aq})$ . The organic layer was washed with distilled water (40 mL) and brine (40 mL) and dried over anhydrous  $\text{MgSO}_4$ . The solvent was removed under reduced pressure, and the product was purified by preparative TLC plates of silica gel 60 (hexane/ethyl acetate 9.5:0.5).

**Diphenyl disulfide (1):** White solid; 25 % yield; m.p. 56 °C, 56-58 °C<sup>[50]</sup>; <sup>1</sup>H-NMR (300 MHz, CDCl<sub>3</sub>): δ=7.19-7.32 (m, 6H; Ar-H), 7.49 (d, *J*=8.64 Hz, 4H; Ar-H); <sup>13</sup>C-NMR (75 MHz, CDCl<sub>3</sub>): δ=127.1 (CH), 127.5 (CH), 137.0 (C); IR (KBr, cm<sup>-1</sup>): 1575, 1475 (C=C); HRMS (ESI): *m/z* calcd. for C<sub>12</sub>H<sub>10</sub>S<sub>2</sub>: 218.0218 [M]<sup>+</sup>; found: 218.0219.

**Bis(4-methylphenyl) disulfide (2):** White solid; 57 % yield; m.p. 43 °C, 43-44 °C<sup>[51]</sup>; <sup>1</sup>H-NMR (300 MHz, CDCl<sub>3</sub>): δ=2.32 (s, 6H; CH<sub>3</sub>), 7.10 (d, *J*=7.89 Hz, 4H; Ar-H), 7.37 (d, *J*=8.04 Hz, 4H; Ar-H); <sup>13</sup>C-NMR (75 MHz, CDCl<sub>3</sub>): δ=21.0 (CH<sub>3</sub>), 128.5 (CH), 129.8 (CH), 133.9 (C), 137.4 (C); IR (KBr, cm<sup>-1</sup>): 1568, 1488 (C=C); HRMS (ESI): *m/z* calcd. for C<sub>14</sub>H<sub>14</sub>S<sub>2</sub>: 246.0513 [M]<sup>+</sup>; found: 246.0553.

**Bis(4-methoxyphenyl) disulfide (3):** Yellow solid; 9 % yield; m.p. 42 °C, 42-43 °C<sup>[52]</sup>; <sup>1</sup>H-NMR (300 MHz, CDCl<sub>3</sub>): δ=3.78 (s, 6H; OCH<sub>3</sub>), 6.81 (d, *J*=8.88 Hz, 4H; Ar-H), 7.38 (d, *J*=8.88 Hz, 4H); <sup>13</sup>C-NMR (75 MHz, CDCl<sub>3</sub>): δ=55.4 (OCH<sub>3</sub>), 114.6 (CH), 128.4 (C), 132.7 (CH), 159.9 (C); IR (KBr, cm<sup>-1</sup>): 1568, 1492 (C=C); HRMS (ESI): *m/z* calcd. for C<sub>14</sub>H<sub>14</sub>O<sub>2</sub>S<sub>2</sub>: 278.0429 [M]<sup>+</sup>; found: 278.0425.

**S-Phenyl benzenethiosulfonate (4):** White solid; 71 % yield; m.p. 38 °C, 36-38 °C<sup>[26]</sup>; <sup>1</sup>H-NMR (300 MHz, CDCl<sub>3</sub>): δ=7.28-7.48 (m, 7H; Ar-H), 7.53-7.58 (m, 3H; Ar-H); <sup>13</sup>C-NMR (75 MHz, CDCl<sub>3</sub>): δ=127.5 (CH), 127.8 (CH), 128.8 (CH), 129.4 (CH), 131.4 (C), 133.6 (CH), 136.5 (CH), 142.9 (C); IR (KBr, cm<sup>-1</sup>): 1575, 1475 (C=C), 1326, 1146 (S=O); HRMS (ESI): *m/z* calcd. for C<sub>12</sub>H<sub>10</sub>O<sub>2</sub>S<sub>2</sub>+H<sup>+</sup>: 251.0194 [M+H]<sup>+</sup>; C<sub>12</sub>H<sub>10</sub>O<sub>2</sub>S<sub>2</sub>+Na<sup>+</sup>: 273.0008 [M+Na]<sup>+</sup>; found: 251.0210, 273.0001.

**S-(4-methylphenyl) 4-methylbenzenesulfonothioate (5):** White solid; 10 % yield; m.p. 72 °C, 72-74 °C<sup>[53]</sup>; <sup>1</sup>H-NMR (300 MHz, CDCl<sub>3</sub>): δ=2.36 (s, 3H; CH<sub>3</sub>), 2.40 (s, 3H; CH<sub>3</sub>), 7.12 (d, *J*=8.1 Hz, 2H; Ar-H), 7.19 (d, *J*=8.5 Hz, 2H; Ar-H), 7.22 (d, *J*=8.4 Hz, 2H; Ar-H), 7.44 (d, *J*=8.2 Hz, 2H; Ar-H); <sup>13</sup>C-NMR (75 MHz, CDCl<sub>3</sub>): δ=21.4 (CH<sub>3</sub>), 21.6 (CH<sub>3</sub>), 124.6 (C), 127.6 (CH), 129.3 (CH), 130.2 (CH), 136.4 (CH), 140.4 (C), 142.0 (C), 144.5 (C); IR (KBr, cm<sup>-1</sup>): 1590, 1488 (C=C), 1323, 1139 (S=O); HRMS (ESI): *m/z* calcd. for C<sub>14</sub>H<sub>14</sub>O<sub>2</sub>S<sub>2</sub>+H<sup>+</sup>: 279.0507 [M+H]<sup>+</sup>; C<sub>14</sub>H<sub>14</sub>O<sub>2</sub>S<sub>2</sub>+Na<sup>+</sup>: 301.0321 [M+Na]<sup>+</sup>; C<sub>14</sub>H<sub>14</sub>O<sub>2</sub>S<sub>2</sub>+K<sup>+</sup>: 317.0061 [M+K]<sup>+</sup>; found: 279.0496, 301.0322, 317.0068.

**S-(4-methoxyphenyl)-4-methoxybenzenesulfonothioate (6):** White solid; 22 % yield; m.p. 85 °C, 84 °C<sup>[26]</sup>; <sup>1</sup>H-NMR (300 MHz, CDCl<sub>3</sub>): δ=3.81 (s, 3H; OCH<sub>3</sub>), 3.85 (s, 3H; OCH<sub>3</sub>), 6.82 (d, *J*=8.5 Hz, 2H; Ar-H), 6.85 (d, *J*=8.6 Hz, 2H; Ar-H), 7.25 (d, *J*=8.4 Hz, 2H; Ar-H), 7.48 (d, *J*=8.9 Hz, 2H; Ar-H); <sup>13</sup>C-NMR (75 MHz, CDCl<sub>3</sub>): δ=55.4 (OCH<sub>3</sub>), 55.7 (OCH<sub>3</sub>), 113.8 (CH), 114.9 (CH), 118.9 (C), 129.9 (CH), 134.9 (C), 138.3 (CH), 162.2 (C), 163.5 (C); IR (KBr, cm<sup>-1</sup>): 1591, 1495 (C=C), 1323, 1139 (S=O), 1261, 1020 (C-O); HRMS (ESI): *m/z* calcd. for C<sub>14</sub>H<sub>14</sub>O<sub>4</sub>S<sub>2</sub>+H<sup>+</sup>: 311.0406 [M+H]<sup>+</sup>; C<sub>14</sub>H<sub>14</sub>O<sub>4</sub>S<sub>2</sub>+Na<sup>+</sup>: 333.0220 [M+Na]<sup>+</sup>; C<sub>14</sub>H<sub>14</sub>O<sub>4</sub>S<sub>2</sub>+K<sup>+</sup>: 348.9959 [M+K]<sup>+</sup>; found: 311.0400, 333.0219, 348.9958.

## Biological assays

**Tubulin assays:** Tubulin assembly<sup>[54]</sup> and inhibition of colchicine binding to tubulin<sup>[55]</sup> were performed as described before. In the assembly assay, the tubulin concentration was 10 μM, and the parameter measured was the extent of assembly after 30 min at 30 °C. In the colchicine binding assay, the tubulin concentration was 1.0 μM, the [<sup>3</sup>H]colchicine concentration was 5.0 μM, and the inhibitor concentration was 5 or 50 μM, as indicated. Incubation was for 10 min at 37 °C, a time point chosen because the control reaction is about 40-60% complete. After the 10 min incubation, samples were diluted with 2 mL of ice cold water, placed on ice, and then filtered through a stack of two DEAE-cellulose filters. In each experiment there were samples without tubulin for determination of background radiolabel retained by the filters and with tubulin but no inhibitor for determination of control binding of colchicine. Typically, the background filters retained about 5% as much radiolabel as the filters with tubulin only. The background radiolabel was subtracted from all samples to determine the % inhibition caused by each potential inhibitor

[(CPM in sample with inhibitor – background CPM) ÷ (CPM in sample without inhibitor – background CPM)] × 100).

**Cell lines and culture conditions:** Tumor cell lines: MCF-7 (ATCC-HTB-22, breast adenocarcinoma); 786-0 (ATCC-CRL-1932, renal cell adenocarcinoma); PC-03 (ATCC-CRL-1435, prostate adenocarcinoma); HEPG2 (ATCC-HB-8065, hepatocellular carcinoma); HT-29 (ATCC-HTB-38, colorectal adenocarcinoma) and MDA-MB-231 (ATCC HTB-26, triple negative breast cancer cells) were cultivated in RPMI-1640 (Roswell Park Memorial Institute Medium). B16-F10 (ATCC CRL-6322, melanoma cells) and non-tumor cell line NIH/3T3 (ATCC CRL-1658 murine fibroblast) were cultivated in DMEM (Dulbecco's Modified Eagle Medium) - Sigma Aldrich®. The culture media were supplemented with 10% fetal bovine serum - Invitrogen® and 1% antibiotics (streptomycin - 100 μg/mL and penicillin 100 IU/mL - Sigma Aldrich®). All cell lines were incubated in a humidified chamber at 37 °C in a 5% CO<sub>2</sub> atmosphere.

**Cell proliferation assay:** The SRB assay was carried out as described by Skehan and coworkers.<sup>[56]</sup> Cell suspensions (3500-7500 cells per well) were seeded in 96 wells plates, incubated and allowed to stabilize for 24 h. The cells were treated with different sample concentrations (0.25; 2.5; 25 and 250 μg/mL) prepared in DMSO and then diluted in culture medium. DMSO (0.25%) alone did not affect cell viability in comparison to the untreated controls. Doxorubicin (DOX) was taken as a positive control only for validation experiments, and used at a ten times lower concentration (Fauldoxo®/LIBBS). The initial optical density (OD) for the SRB assay was measured at the same moment as compounds were added to the samples (Time 0) and after a 48 h treatment, (exceptionally for line cell 786-0, it was performed independent experiments at time periods of 12, 24 and 48h). The OD of each well was determined by measuring at 540 nm using a microplate reader (SpectraMax 190 microplate reader - Molecular Devices), and the absorbance values were used to determine the percentage of cell growth, calculated using the software Soft Max Pro 6.3 as described by Monks and coworkers.<sup>[57]</sup> The results were expressed as a curve of cell growth versus compound concentration. GI<sub>50</sub> values (50% cell growth inhibition, TGI (total cell growth inhibition) and LC<sub>50</sub> (50% cell death) were determined by non-linear regression analysis using data graphic software (Origin version 6.0). This assay was performed in three independent experiments, and the results are expressed in molarity. The compounds were classified as either active (GI<sub>50</sub><10 μM), moderately active (GI<sub>50</sub> between 10 and 100 μM), or inactive (GI<sub>50</sub>>100 μM).<sup>[58]</sup> Subsequently, compound **6** was evaluated by the SRB cytotoxicity assay against the cell line 786-0 (ATCC-CRL-1932) in treatment periods of 12, 24 and 48 h.

**Morphological analysis:** The AO/EB staining assay permits the identification of viable, apoptotic, and necrotic cells. It was used to evaluate death induction in 786-0 cells (ATCC-CRL-1932) after treatment for periods of 24 and 48 h with compound **6** at the same concentrations used for cytotoxicity tests. In order to carry out this assay, the cells were collected and resuspended in phosphate-buffered saline (PBS). The slides were prepared with 10 μL of the cell suspension and 1 μL of the stain mixture containing ethidium bromide (100 μg/mL) and acridine orange (100 μg/mL). Three experiments were performed, and 100 treated cells were analyzed by fluorescence, 400x magnification (Olympus BX41). For the image acquisition we used excitation wave of 420-490 nm and barrier filter of 520 nm. Morphological alterations were also evaluated by optical microscopy after treatment with compound **6** at concentrations near the values of the GI<sub>50</sub>, TGI and LC<sub>50</sub>, for 24 or 48 h.

**Quantification of caspase-3 by flow cytometry:** The assay was performed using the antibody PE Rabbit Anti-Active Caspase-3 (BD Pharmingen). The cells of the line 786-0 (ATCC-CRL-1932) were seeded in 6 well plates (4x10<sup>5</sup>/well), and they were allowed to stabilize for 24 h. The cells were treated with compound **6** at concentrations near the GI<sub>50</sub>, TGI and, LC<sub>50</sub> values for 24 or 48 h. After each incubation period, the cells were collected, washed twice with cold PBS, fixed, and permeabilized with BD Cytofix/Cytoperm for 20 min. Then, the cells were

centrifuged, washed twice with BD Perm/Wash and incubated on ice for 30 min with the antibody Rabbit Anti-Active Caspase-3 in the dark to prevent degradation. The assay was performed in triplicate, and caspase-3 quantification was carried out by flow cytometry in the channel FL-2 (Cytometer BD Accuri™ C6, BD Bioscience), and 10,000 events were recorded.

**Cell cycle:** The experiment was executed by flow cytometry using the reagent 7-aminoactinomycin D (7-AAD) (Biolegend). This reagent is a DNA intercalating agent and emits fluorescence proportional to the amount of cell DNA. The 786-0 cells (ATCC-CRL-1932) were seeded in 6 well plates (4x10<sup>5</sup>/well) and incubated for 24 h. After treatments for 24 or 48 h with compound **6** at the GI<sub>50</sub>, TGI, and LC<sub>50</sub> concentrations, the cells were collected, washed twice with cold PBS and fixed with 70% ethanol at 4 °C for at least 30 min. Following centrifugation, the ethanol was removed. Then, the cells were washed twice with cold PBS, incubated for 30 min in a solution containing 0.1 % Triton X-100, 0.1 mM EDTA and 50 µg/mL of RNase in PBS for membrane lysis, and 7-AAD was added with the cell remnants kept on ice in the dark. The assay was performed in triplicate, and fluorescence acquisition was obtained in a flow cytometer in channel FL-3, with 10,000 events recorded.

**Statistical analysis:** For all experiments, data were presented as means±standard error of the mean (SEM). The results of experiments in which morphological evaluation, quantification of caspase-3, and cell cycle data were obtained, analysis was performed using GraphPad Prism software (version 5.0; GraphPad Software, Inc., La Jolla, CA, USA). Significant differences between the treatments and control samples was assessed using ANOVA/Dunnett, ANOVA/Tukey, or Student's unpaired t-test with P values <0.01 or <0.05 being regarded as statistically significant.

#### Molecular modeling

Protein coordinates used for modeling were taken from PDB 5LYJ, a 2.4 Å resolution co-crystal of CSA4 bound in the colchicine site. Energy refinement of CSA4 bound in the colchicine site was performed as previously described.<sup>[39]</sup> The MacroModel minimization module in Maestro v2016-1 (Schrödinger, LLC, New York, NY) was used to prepare compound **6** using the OPLS3 forcefield, with a distance-dependent dielectric = 1.0, until the maximum derivative was < 0.001 kcal/Å. The Glide module in Maestro (Schrödinger, LLC, New York, NY) was used to score the energy refined model of bound CSA4 in extra precision (XP) mode using the OPLS3 force field. For compound **6**, a docking grid was generated using bound CSA4 as the reference model. Subsequently, XP Glide docking was used in flexible ligand sampling mode, OPLS3 forcefield, and using default settings (but with the distance dielectric set to 1.0, and the maximum number of minimization steps set to 10,000) to generate the binding pose for the compound.

#### Acknowledgements

**Acknowledgements Text.** The authors owe a debt of gratitude to the following Brazilian research agencies: FUNDECT-MS, CAPES, PROPP-UFMS and, CNPq for financial support and scholarships.

#### Disclaimer

This research was supported in part by the Developmental Therapeutics Program in the Division of Cancer Treatment and Diagnosis of the National Cancer Institute, which includes federal funds under Contract No. HHSN261200800001E. The content of this publication does not necessarily reflect the views

or policies of the Department of Health and Human Services, nor does mention of trade names, commercial products, or organizations imply endorsement by the U.S. Government.

#### Conflict of interest

The authors declare no conflict of interest.

**Supporting information:** Supplementary data (spectral data for the synthesized compounds) associated with this article can be found.

#### Conflict of interest

The authors declare no conflict of interest.

**Keywords:** disulfide • thiosulfonate • tubulin • 786-0 cell • caspase-3

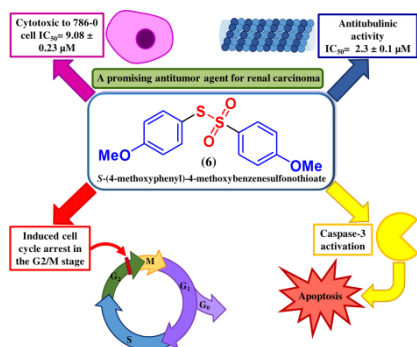
#### References:

- [1] G. I. Evan, K. H. Vousden, *Nature* **2001**, *411*, 342-348.
- [2] G. H. Williams, K. Stoeber, *J. Pathol.* **2012**, *226*, 352-364.
- [3] M. De Falco, A. De Luca, *Curr. Pharm. Des.* **2010**, *16*, 1417-1426.
- [4] R. W. Johnstone, A. A. Ruefli, S. W. Lowe, *Cell* **2002**, *108*, 153-164.
- [5] A. Kamb, S. Wee, C. Lengauer *Nat. Rev. Drug. Discov.* **2006**, *6*, 115-120.
- [6] G. Housman, S. Byler, S. Heerboth, K. Lapinska, M. Longacre, N. Snyder, S. Sarkar *Cancers* **2014**, *6*, 1769-1792.
- [7] B. Ljungberg, L. Albiges, K. Bensalah, A. Bex, R. H. Giles, M. Hora, M. A. Kuczyk, T. Lam, L. Marconi, A. S. Merseburger, T. Powles, M. Staehler, A. Volpe, S. Dabestani, S. F.-P. Montes, F. Hofmann, R. Tahbaz, Guidelines on renal cell carcinoma, European Association of Urology 2017. [http://uroweb.org/wp-content/uploads/10-Renal-Cell-Carcinoma\\_2017\\_web.pdf](http://uroweb.org/wp-content/uploads/10-Renal-Cell-Carcinoma_2017_web.pdf). Accessed 03 August 2019.
- [8] M. Pljesa-Ercegovic, J. Mimic-Oka, D. Dragicevic, A. Savic-Radojevic, M. Opacic, S. Pljesa, R. Radosavljevic, T. Simic, *Urol. Oncol.: Semin. Orig. Invest.* **2008**, *26*, 175-181.
- [9] Y. Xiao, D. Meierhofer, *Int. J. Mol. Sci.* **2019**, *20*, 3672.
- [10] M. Smith, R. Hunter, N. Stellenboomb, D. A. Kusza, M. I. Parker, A. N. H. Hammouda, G. Jackson, C. H. Kaschula, *Biochim. Biophys. Acta* **2016**, *1860*, 1439-1449.
- [11] C. Mignogna, S. Staibano, V. Altieri, G. De Rosa, G. Pannone, A. Santoro, R. Zamparese, M. D'Armiento, R. Rocchetti, E. Mezza, M. Nastì, V. Strazzullo, V. Montanaro, M. Mascolo, P. Bufo, *BMC Cancer* **2006**, *6*, 293.
- [12] N. Walsh, A. Larkin, S. Kennedy, L. Connolly, J. Ballot, W. Ooi, G. Gullo, J. Crown, M. Clynes, L. O'Driscoll, *BMC Urol.* **2009**, *9*, 6.
- [13] G. Keller, A. V. Schally, A. Nagy, G. Halmos, B. Baker, J. B. Engel, *Cancer* **2005**, *104*, 2266-2274.
- [14] W. Y. Kim, W. G. Kaelin, *J. Clin. Oncol.* **2004**, *22*, 4991-5004.
- [15] S. Vanharanta, W. Shu, F. Brenet, A. A. Hakimi, A. Heguy, A. Viale, V. E. Reuter, J. J. Hsieh, J. M. Scandura, J. Massagué, *Nat Med.* **2013**, *19*, 50-56.
- [16] E. G. Barbosa, L. A. S. Bega, A. Beatriz, T. Sarkar, E. Hamel, M. S. Do Amaral, D. P. De Lima, *Eur. J. Med. Chem.* **2009**, *44*, 2685-2688.
- [17] E. A. Dos Santos, E. Hamel, R. Bai, J. C. Burnett, C. S. S. Tozatti, D. Bogo, R. T. Perdomo, A. M. M. Antunes, M. M. Marques, M. F. C. Matos, D. P. De Lima, *Bioorg. Med. Chem. Lett.* **2013**, *13*, 4669-4673.
- [18] D. Rotili, A. De Luca, D. Tarantino, S. Pezzola, M. Forgione, B. M. Della Rocca, M. Falconi, A. Mai, A. M. Caccuri, *Eur. J. Med. Chem.* **2015**, *89*, 156-171.
- [19] C.-C. Xu, J.-J. Wu, T. Xu, C.-H. Yao, B.-Y. Yu, J.-H. Liu, *Eur. J. Med. Chem.* **2016**, *123*, 763-768.

- [20] X. Ma, M. Laramie, M. Henary, *Bioorg. Med. Chem. Lett.* **2018**, *28*, 509-514.
- [21] V. Siyo, G. Schäfer, R. Hunter, A. Grafov, I. Grafova, M. Nieger, A. A. Katz, M. I. Parker, C. H. Kaschula, *Molecules* **2017**, *22*, 892-911.
- [22] J. Pan, K. S. Carroll, *ACS Chem. Biol.* **2013**, *8*, 1110-1116.
- [23] G. Kong, K. C. Kain, I. Crandall, R. F. Langler, *Sulfur Lett.* **2003**;26:149-154.
- [24] K. M. Khan, M. Taha, F. Naza, M. Khana, F. Rahim, Samreen, S. Perveen, M. I. Choudhary, *Med. Chem.* **2011**, *7*, 704-710.
- [25] F. J. Baerlocher, M. O. Baerlocher, C. L. Chaulk, R. F. Langler, S. L. MacQuarrie, *Aust. J. Chem.* **2000**, *53*, 399-402.
- [26] E. A. Dos Santos, F. H. M. Gonçalves, P. C. Prado, D. Y. Sasaki, D. P. De Lima, M. L. R. Macedo, *Int. J. Mol. Sci.* **2012**, *13*, 15241-15251.
- [27] H. Wang, Y. Mao, A. Y. Chen, N. Zhou, E. J. LaVoie, L. F. Liu, *Biochemistry* **2001**, *40*, 3316-3323.
- [28] T. Schmid, J. S. Blees, M. M. Bajer, J. Wild, L. Pescatori, G. C. Crucitti, L. Scipione, R. Costi, C. J. Henrich, B. Brüne, N. H. Colburn, R. Di Santo, *PLoS ONE* **2016**, *11*, e0151643.
- [29] Q. Zhang, Y. Peng, X. I. Wang, S. M. Keenan, S. Arora, W. J. Welsh, *J. Med. Chem.* **2007**, *50*, 749-754.
- [30] G. La Regina, M. C. Edler, A. Brancale, S. Kandil, A. Coluccia, F. Piscitelli, E. Hamel, G. De Martino, R. Matesanz, J. F. Díaz, A. I. Scovassi, E. Prosperi, A. Lavecchia, E. Novellino, M. Artico, R. Silvestri, *J. Med. Chem.* **2007**, *50*, 2865-2874.
- [31] G. R. Pettit, J. K. Srirangam, J. Barkoczy, M. D. Williams, K. P. M Durkin, M. R. Boyd, E. Hamel, R. Bai, J. M. Schmidt, J.-C. Chapuis, *Anti-Cancer Drug Des.* **1995**, *10*, 529-544.
- [32] D. G. I. Kingston, A. G. Chaudhary, M. D. Chordia, M. Gharpure, A. A. L. Gunatilaka, P. I. Higgs, J. M. Rimoldi, L. Samala, P. G. Jagtap, P. Giannakakou, Y. Q. Jiang, C. M. Lin, E. Hamel, B. H. Long, C. R. Fairchild, K. A. Johnston, *J. Med. Chem.* **1998**, *41*, 3715-3726.
- [33] T. L. Nguyen, C. McGrath, A. R. Hermone, J. C. Burnett, D. W. Zaharevitz, B. W. Day, P. Wipf, E. Hamel, R. A. Gussio, *J. Med. Chem.* **2005**, *48*, 6107-6116.
- [34] A. Herman-Antosiewicz, S. V. Singh, *Mutat. Res.* **2004**, *555*, 121-131.
- [35] D. N. Gunadharini, A. Arunkumar, G. Krishnamoorthy, R. Muthuvel, M. R. Vijayababu, P. Kanagaraj, N. Srinivasan, M. M. Aruldas, J. Arunakaran, *Cell Biochem. Funct.* **2006**, *24*, 407-412.
- [36] F. Gao, H. Zhai, M. Jin, G. Chu, H. Duan, C. Li, *Synthesis* **2011**, *22*, 3635-3638.
- [37] P. C. Carvalho, E. A. Santos, B. U. C. Schneidera, R. Matuo, J. R. Pesarini, A. L. Cunha-Laura, A. C. D. Monreal, D. P. Lima, A. C. M. B. Antonioli, R. J. Oliveira, *Environ. Toxicol. Pharmacol.* **2015**, *40*, 715-721.
- [38] L. Yi, Q. Su, *Food Chem. Toxicol.* **2013**, *57*, 362-370.
- [39] A. Dasgupta, M. Nomura, R. Shuck, J. Yustein, *Int. J. Mol. Sci.* **2017**, *18*, 23-42.
- [40] G. Ichim, S. W. Tait, *Nat. Rev. Cancer* **2016**, *16*, 539-548.
- [41] D. Xiao, J. T. Pinto, G. G. Gundersen, I. B. Weinstein, *Mol. Cancer Ther.* **2005**, *4*, 1388-1398.
- [42] C. Cerella, M. Dicato, C. Jacob, M. Diederich, ion of garlic-derived organic sulfur compounds. *Anticancer Agents Med. Chem.* **2011**, *11*, 267-271.
- [43] M. Suffness, J. M. Pezzuto, *Assays related to cancer drug discovery in Methods in Plant Biochemistry, Assays for Bioactivity*, Vol. 6 (Ed.: K. Hostettmann), Academic Press, London, **1990**, pp. 71-133.
- [44] R. Griffiths, W. W. Wong, S. P. Fletcher, L. Z. Penn, R. F. Langle, *Aust. J. Chem.* **2005**, *58*, 128-136.
- [45] K. M. Hajra, J. R. Liu, *Apoptosis* **2004**, *9*, 691-704.
- [46] M. A. Jordan, L. Wilson, *Nat. Rev. Cancer* **2004**, *4*, 253-265.
- [47] V. J. Raja, K. H. Lim, C. O. Leong, T. S. Kam, T. D. Bradshaw, *Invest. New Drugs.* **2014**, *32*, 838-850.
- [48] P. M. Checchi, J. H. Nettles, J. Zhou, J. P. Snyder, H. C. Joshi, *Trends Pharmacol. Sci.* **2003**, *24*, 361-365.
- [49] M. J. Pilat, M. J. LoRusso, *J. Cell. Biochem.* **2006**, *99*, 1021-1039.
- [50] H. Kutuk, N. Turkoz, *Phosphorus Sulfur Silicon Relat. Elem.* **2011**, *186*, 1515-1522.
- [51] S. P. Sharma, M. V. S. Suryanarayana, A. K. Nigam, A. S. Chauhan, L. N. S. Tomar, *Catal. Commun.* **2009**, *10*, 905-912.
- [52] C. C. Silveira, S. R. Mendes, *Tetrahedron Lett.* **2007**, *48*, 7469-7471.
- [53] S. Oae, T. Takata, Y. H. Kim, *Tetrahedron* **1981**, *37*, 37-44.
- [54] E. Hamel, *Cell Biochem. Biophys.* **2003**, *38*, 1-22.
- [55] P. Verdier-Pinard, J.-Y. Lai, H.-D. Yoo, J. Yu, B. Márquez, D. G. Nagle, M. Nambu, J. D. White, J. R. Falck, W. H. Gerwick, B. W. Day, E. Hamel, *Mol. Pharmacol.* **1998**, *53*, 62-76.
- [56] P. Skehan, R. Storeng, D. Sundiero, A. Monks, J. McMahon, D. Vistica, J. T. Warren, H. Bokesch, S. Kenney, M. R. Boyd, *J. Natl. Cancer Inst.* **1990**, *82*, 1107-1112.
- [57] A. Monks, D. Scudiero, P. Skehan, R. Shoemaker, K. Paull, D. Vistica, C. Hose, J. Langley, P. Cronise, A. Vaigro-Woiff, M. G. Goodrich, H. Campbell, J. Mayo, M. Boyd, *J. Natl. Cancer Inst.* **1991**, *83*, 757-766.
- [58] M. M. Da Silva MM, M. Comin, T. S. Duarte, M. A. Foglio, J. E. De Carvalho, M. C. Do Vieira, A. S. Formagio, *Molecules* **2015**, *20*, 5360-5373.

## Entry for the Table of Contents

Insert graphic for Table of Contents here.



**Repurposing a diaryl thiosulfonate:** S-(4-methoxyphenyl)-4-methoxybenzenesulfonothioate (**6**) exhibited antitubulin activity. Compound **6** showed antiproliferative activity against the 786-0 cell line. Compound **6** induces morphological alterations and death in 786-0 cell line. Compound **6** activates caspase-3. Compound **6** induces G2/M phase cell cycle arrest in 786-0 cells.